

breakthroughs in either of these areas would provide powerful new tools which could be expected to find many unusual applications.

References and Notes

1. *Laser Focus* **18**, 69 (January 1982).
2. F. Hillenkemp *et al.*, Eds., *Lasers in Biology and Medicine* (Plenum, New York, 1981).
3. M. W. Berns *et al.*, *Science* **213**, 505 (1981).
4. R. W. Waynant and L. Goldman, *Appl. Opt.* **19**, 3388 (1980).
5. *Laser Focus* **17**, 64 (January 1981).
6. C. M. Davis, *Fiberoptic Technol.* (January 1982), p. 112.
7. M. Richardson, *IEEE J. Quantum Electron.* **QE-17**, 1598 (1981).
8. R. L. Fork, B. I. Greene, C. V. Shank, *Appl. Phys. Lett.* **38**, 104 (1981).
9. *Phys. Today* **33**, 25 (November 1980); S. S. Carschan, *Electro-Opt. Syst. Des.* (August 1981), p. 63; K. G. P. Sultzmans and P. Hammerling, *Laser Focus* **17**, 66 (March 1981); *ibid.* **18**, 85 (January 1982).
10. T. F. Deutsch, D. J. Ehrlich, R. M. Osgood, Jr., *Appl. Phys. Lett.* **35**, 175 (1979).
11. R. Solanki, P. K. Boyer, J. E. Mahan, G. J. Collins, *ibid.* **32**, 254 (1978).
12. C. P. Christensen and K. M. Lakin, *ibid.*, p. 254.
13. V. Baranauskas, C. I. Z. Mammana, R. E. Klinger, J. E. Green, *ibid.* **36**, 930 (1980).
14. S. D. Allen and M. Bass, *J. Vac. Sci. Technol.* **16**, 431 (1979).
15. G. Leyendecker, D. Bauerle, P. Geittner, H. Lydtin, *Appl. Phys. Lett.* **39**, 921 (1981).
16. D. J. Ehrlich, R. M. Osgood, Jr., T. F. Deutsch, *ibid.* **36**, 698 (1980).
17. ———, *ibid.* **38**, 1018 (1981).
18. T. F. Deutsch, J. C. C. Fan, G. W. Turner, R. L. Chapman, D. J. Ehrlich, R. M. Osgood, Jr., *ibid.*, p. 144.
19. D. J. Ehrlich, R. M. Osgood, Jr., T. F. Deutsch, *ibid.*, p. 399.
20. H. Brody, *Laser Focus* **17**, 47 (August 1981).
21. H. G. Craighead and R. E. Howard, *Appl. Phys. Lett.* **39**, 532 (1981).
22. N. Lee, Y. Kohanzadeh, P. Shepherd, and S. Chao, paper presented at the SPIE (Society of Photographic Instrumentation Engineers) Technical Symposium, Los Angeles, January 1982.
23. M. A. Bosch, *Appl. Phys. Lett.* **40**, 8 (1982).
24. M. Mansuripur and G. A. N. Connell, paper presented at the SPIE Technical Symposium, Los Angeles, January 1982.
25. D. Kowalski, D. Curry, L. Klinger, paper presented at the SPIE Technical Symposium, Los Angeles, January 1982.
26. G. J. Ammon and C. W. Reno, paper presented at the SPIE Technical Symposium, San Diego, August 1981.
27. R. L. Beyer, *Opt. Quantum Electron.* **7**, 147 (1975).
28. F. E. Hoge, R. N. Swift, E. B. Frederick, *Appl. Opt.* **19**, 871 (1980).
29. C. S. Gardner, C. F. Sechrist, Jr., J. D. Shelton, *ibid.*, p. A192.
30. F. E. Hoge and R. N. Swift, *ibid.*, p. 3269.
31. J. P. deNeufville, A. Kasdan, R. J. L. Chimenti, *ibid.* **20**, 1279 (1981).
32. M. Endemann and R. L. Beyer, *ibid.*, p. 3211.
33. C. A. Brau, *Laser Focus* **17**, 48 (May 1981); A. Szoke, *IEEE J. Quantum Electron.* **QE-17**, 1326 (1981).
34. R. W. Waynant and R. C. Elton, *Proc. IEEE* **64**, 1092 (1976); C. K. Rhodes, paper presented at the Conference on Lasers and Electro-optics, Washington, D.C., June 1981.

Sedimentation Field Flow Fractionation: Applications

J. J. Kirkland and W. W. Yau

High-resolution separations of a wide range of inorganic and organic colloids and soluble macromolecules in the molecular weight range 10^6 to 10^{13} can be carried out by sedimentation field flow fractionation (SFFF). In SFFF, which

resolution fractograms similar to chromatograms, with species eluting in the order of increasing mass or particle density. Separations take place as a result of physical properties (molecular weight or mass) rather than chemical properties of

Summary. Sedimentation field flow fractionation is a powerful, new, high-resolution separation method for a wide variety of colloids, micelles, particulates, and soluble macromolecules of biological interest. Advances in instrumentation allow sedimentation field flow fractionation operation with rotor speeds up to 32,000 revolutions per minute ($\sim 85,000$ gravities), which permits separation of materials as small as 5×10^5 molecular weight, depending on sample density. Compared to conventional centrifugation techniques, the gentle, mass-separating sedimentation field flow fractionation method is capable of higher resolution in shorter times.

may be characterized as a one-phase chromatographic method, separations are performed with a single, continuously flowing mobile phase in a very thin, open channel under the influence of an external centrifugal force field (1, 2). Sample retention takes place by the redistribution of components from fast- to slow-moving mobile phase streams near the wall of the channel because of the influence of this external force field. As a result, the SFFF method produces high-

the solute. Based on the molecular weight or mass information from SFFF separations, other physical properties can be deduced, including Stokes particle diameters and diffusivity (3, 4).

For field flow fractionation (FFF) in general, the applied force field can be of any type that interacts with sample components and causes them to move perpendicular to the flow direction in the open channel. For example, the field can be a temperature gradient as in thermal

FFF, electrical potential as in electrical FFF, or hydraulic potential as in cross-flow FFF (5). Although there is some overlap in the FFF subtechniques, they are generally complementary in potential applications (Fig. 1). Some form of FFF is generally available for the high-resolution fractionation of components in the medium to ultrahigh molecular weight range 10^3 to 10^{16} .

The most highly developed of the various FFF subtechniques is SFFF. While separating species on the basis of differences in mass, SFFF also has the highest intrinsic resolving power. It has been used for characterizing polymer latices, for both inorganic and organic colloids and pigments, viruses, liposomes, and other vesicles, and for DNA, RNA, and other polynucleotides of biochemical interest. Some biochemical applications of SFFF are given in this article. Equipment for SFFF is similar to that used in liquid chromatography except for a special channel and a means of supplying the necessary centrifugal force.

Retention in SFFF

Fractionation in SFFF results from a sedimentation equilibrium being superimposed on a steep mobile-phase velocity gradient, the combined effect of which results in a large discrimination of one particle mass from another. Separations are carried out in an open channel formed between two closely spaced concentric surfaces with a very narrow gap (for example, 0.25 millimeter) (Fig. 2a).

J. J. Kirkland and W. W. Yau are staff scientists at the E. I. du Pont de Nemours & Company, Central Research and Development Department Experimental Station, Wilmington, Delaware 19898.

The sample is injected into this open channel, which is shaped like a ribbon or belt suspended in a centrifuge. Usually the sample is injected into the rotating channel while the mobile phase flow is interrupted temporarily. In a preequilibration or relaxation step, the centrifugal force causes sample components to be pushed toward the wall regions. Sample particles that are more dense than the mobile phase collect next to the outer wall; particles of lower density go to the inner wall.

Buildup of sample concentration near the outer wall is resisted by normal diffusion of the particles in the opposite direction. Smaller sample components have higher diffusion rates and will accumulate in a layer that extends farther away

from the outer wall than layers of larger particles do. This effect is illustrated in Fig. 2b where ℓ_A and ℓ_B are the characteristic layer thicknesses representing the mean of the exponential population profile of the smaller and larger components, respectively. Distinct species assume different characteristic layer thicknesses within the channel. The highest concentration of sample components is near the wall, and this population decreases exponentially with distance from the wall. In Fig. 2b, liquid mobile phase is pumped steadily through the channel, and a parabolic flow velocity profile is formed. Movement of particles closer to the wall puts them in regions of slower flow. Solvent molecules and very small particles that are not influenced by the

external force field travel in all flow streams at an average linear velocity equal to that of the carrier liquid and elute first (Fig. 2c; see fractogram at the bottom of the figure); components of increasing mass follow (Fig. 2d). The resulting fractogram, resembling a chromatogram, provides quantitative information on the mass or molecular weights of sample constituents.

In SFFF retention, it has been shown that

$$\ell = \frac{R_0 T}{M \omega^2 r (\Delta \rho / \rho_s)} = \frac{6kT}{\pi d_p^3 \omega^2 r \Delta \rho} \quad (1)$$

where R_0 is the gas constant (8.31×10^7 g · cm²/sec² · deg · mole); T is the absolute temperature (Kelvin); M is the molecular weight of the solvated macromolecules or particle mass in grams per mole; ω is the centrifuge angular velocity in radians per second; r is the radial distance, in centimeters, from the centrifuge rotation axis to the channel; $\Delta \rho$ is the density difference between the sample and the mobile phase, and ρ_s is the density of the sample component (both in grams per cubic centimeter); and $M = N(\pi d_p^3/6)\rho_s$, where N is Avogadro's number (6.022×10^{23} mole⁻¹), k is Boltzmann's constant (1.38×10^{-16} g · cm²/sec² · deg), and d_p is the spherical particle diameter in centimeters (δ).

In SFFF, the average downstream migration velocity of retained sample components is smaller than the average velocity of the unretained liquid carrier. Thus, the characteristic retention ratio, R , is equal to or less than 1 in all SFFF separations

$$R = \frac{\bar{v}}{\bar{v}_0} = \frac{V_0}{V_R} = \frac{t_0}{t_R} \leq 1 \quad (2)$$

where \bar{v} and \bar{v}_0 are the mean downstream velocities of the particles and the carrier liquid, respectively, V_0 is the channel void volume, V_R is the retention volume of the eluted species, and t_0 and t_R are the solvent and particle retention times, respectively. The retention ratio R is related to ℓ values by

$$R = 6\lambda[\coth(1/2\lambda) - 2\lambda] \quad (3)$$

with

$$\lambda = \ell/W \quad (4)$$

where W is the channel thickness and $\coth(1/2\lambda)$ is the hyperbolic cotangent of $(1/2\lambda)$. For component peaks eluting at least two channel volumes beyond the void volume peak ($R < 0.3$),

$$R \approx 6\lambda \quad (5)$$

Since useful retention in FFF is usually maintained at or less than $R = 0.3$, this simplified approximation is satisfactory

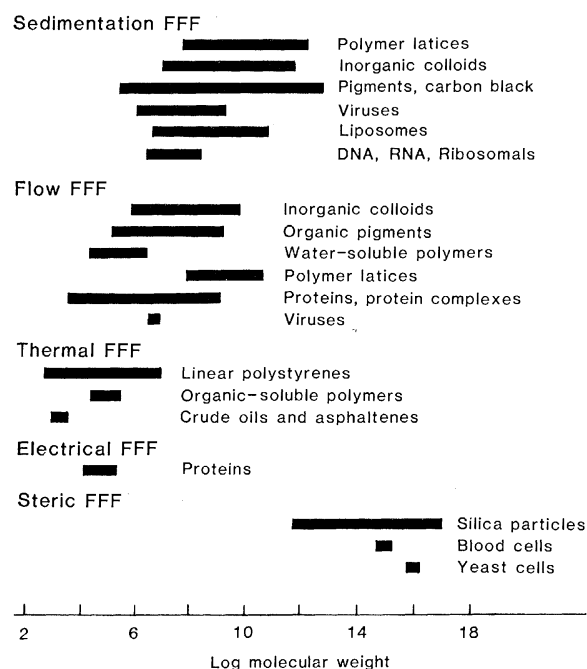


Fig. 1. Applications of field flow fractionation.

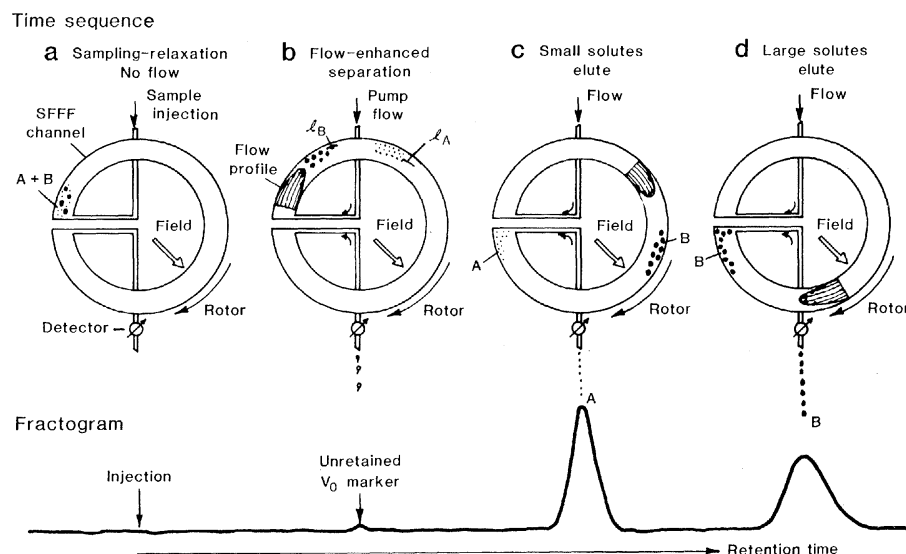


Fig. 2. Development of SFFF separation.

for most situations to relate experimentally measurable R values to SFFF operating parameters through Eqs. 3 and 4. The upper limit of particle size that can be quantitatively analyzed by SFFF is usually in the 1- to 2-micrometer range, when the particle diameter approaches the ℓ value. Verification of SFFF retention expressions and the effects of operating parameters have been documented by Giddings *et al.* (7). Under carefully controlled conditions, particle size accuracy and precision can be obtained in the range of 1 percent.

Although the highest resolution is obtained with a constant force field (rotor speed), SFFF separations have many limitations in this mode. (i) The dependence of SFFF retention on particle diameter is nonlinear (Eqs. 1 to 5), and this makes it inconvenient for converting SFFF fractograms to a quantitative particle size distribution. (ii) Constant-field SFFF provides uneven particle size resolution across the fractogram. (iii) The range of particle separation that is possible in a single constant-field SFFF separation is very narrow, corresponding to less than a twofold difference in particle diameter; this presents a problem for the analysis of samples with wide particle size (or mass) distribution. (iv) The highly broadened peaks of late eluting species in constant-field SFFF can pose a detection problem. These disadvantages are exemplified in Fig. 3a, which shows a mixture of five polystyrene latex standards fractionated with two different centrifugal force fields. At 1710 revolutions per minute, only the largest particle component of the sample mixture (peak E) is completely resolved from the other particles. At 4360 rev/min, the larger particles are resolved, but only at excessively long retention times; the two smallest components still overlap.

Figure 3a also demonstrates the poor dynamic range of constant-field SFFF separation. A single force field is insufficient to resolve all five components in a reasonable analysis time. This fractogram also illustrates the nonuniform resolution by particle diameter—larger particles are very much better resolved than smaller ones. In Fig. 3b, the graphs of molecular or particle mass plotted against retention time show the expected linear relation (Eqs. 1 to 5) for particle mass, but this leads to the nonlinear dependence of particle diameter.

A method of programmed reduction of gravitational field in SFFF has been found effective in overcoming these difficulties (3, 8, 9). In a time-delayed exponential SFFF method (TDE-SFFF) after sample injection and relaxation, the ini-

tial force field G_0 is maintained after the start of mobile phase flow for a time period equal to τ , and then the force field is allowed to decay exponentially at a rate corresponding to the same time constant τ . In TDE-SFFF, retention assumes a simple log-linear relation

$$t_R = \tau \ln(M/\alpha) = 3\tau \ln(d_p/\beta) \quad (6)$$

where

$$\alpha = \frac{6R_0T\tau}{et_0G_0W(\Delta\rho/\rho_s)}$$

$$\beta = \left(\frac{36kT\tau}{\pi et_0G_0W\Delta\rho} \right)^{1/3}$$

$G_0 = \omega_0^2 r$ and $e = 2.718$, the natural logarithm base.

The desirable features of TDE-SFFF are illustrated by the fractogram in Fig. 4 for five polystyrene latex standards that are completely separated in about 22 minutes with easily detected bands of approximately equal width. Figure 5 shows the expected linear relation between the logarithm of particle diameter d_p and the retention time t_R for these data. The solid-line plots in Fig. 5 show the expected slope changes on the log-linear plot as τ values vary according to Eq. 6. Thus, by varying the exponential decay constant τ , one can obtain a trade-off between analysis time and resolution. According to Eq. 6, changes in the other SFFF parameters (that is, initial force field G_0 , channel thickness W , mobile phase density ρ or $\Delta\rho$, and flow rate F)

should change the intercept, but not the slope, of the log-linear retention relation. This is illustrated in Fig. 5 for a different flow rate, which results in the dashed line that is displaced but remains parallel to the solid line at $\tau = 4$ minutes. Increases in G_0 , $\Delta\rho$, and W , and a decrease in F all result in greater retention in TDE-SFFF, and therefore are better suited to separate small particles.

Comparison of SFFF with Other Methods

Centrifugation. Since SFFF is a true sedimentation equilibrium process, it can provide rigorous measurements of solute molecular weight or particulate mass. In contrast, most conventional centrifugal methods are based on sedimentation velocity, which is affected by the viscosity of the liquid medium and the shape of the solutes or particulates. While sedimentation equilibrium is sometimes reached in density gradient centrifugation, such methods are tedious and time-consuming. Owing to fundamental differences in the basis of separation, density gradient equilibrium sedimentation provides information only on density, whereas the sedimentation equilibrium approach in SFFF gives particle size information as well.

Higher resolutions and shorter analysis times can be provided by SFFF than by conventional centrifugation techniques because of the different separa-

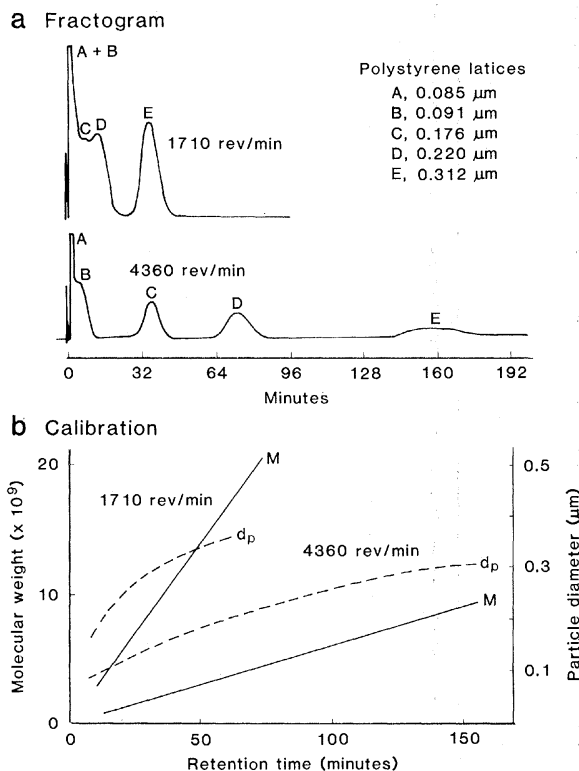


Fig. 3. Constant force field SFFF. (a) Fractograms at two rotor speeds. (b) Calibration curves for molecular weight (—) and particle diameter (---). Channel, 57 by 2.54 by 0.0254 cm. Mobile phase, 0.1 percent FL-70 surfactant. Flow rate, 2.0 ml/min. Relaxation, 10 minutes at ω_0 . Sample, 25 μl , 0.1 percent of 0.085- μm , 0.09 percent of 0.091- μm , and 0.04 percent each of 0.176-, 0.220-, and 0.312- μm polystyrene latex standards. Ultraviolet detector, 300 nm. Temperature, 22°C.

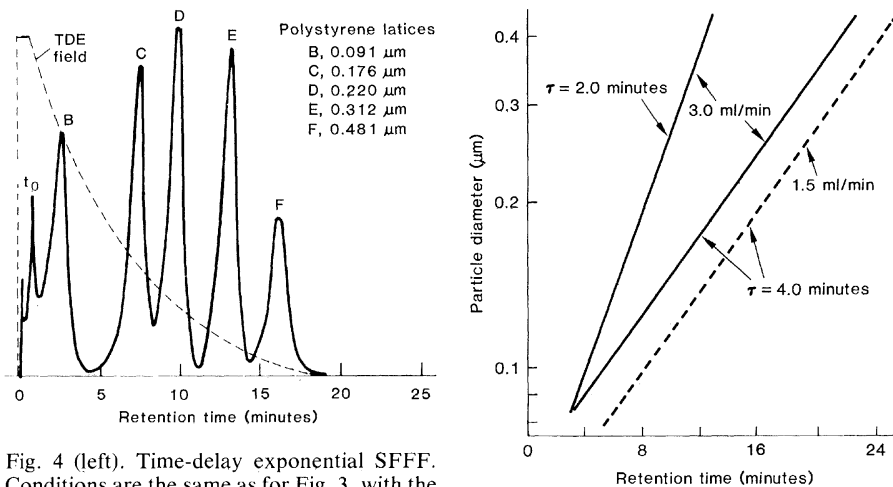


Fig. 4 (left). Time-delay exponential SFFF. Conditions are the same as for Fig. 3, with the following exceptions. Flow rate, 3.0 ml/min. Initial rotor speed, 10,000 rev/min. Decay time constant $\tau = 4.76$ minutes. Sample, 10 μl , 0.09 percent of 0.091- μm , 0.04 percent each of 0.176-, 0.220-, and 0.312- μm , and 0.05 percent of 0.418- μm polystyrene latex standards. Fig. 5 (right). Effect of time-delay exponential separation parameters on plot of log particle diameter versus retention time. Conditions are the same as for Fig. 4.

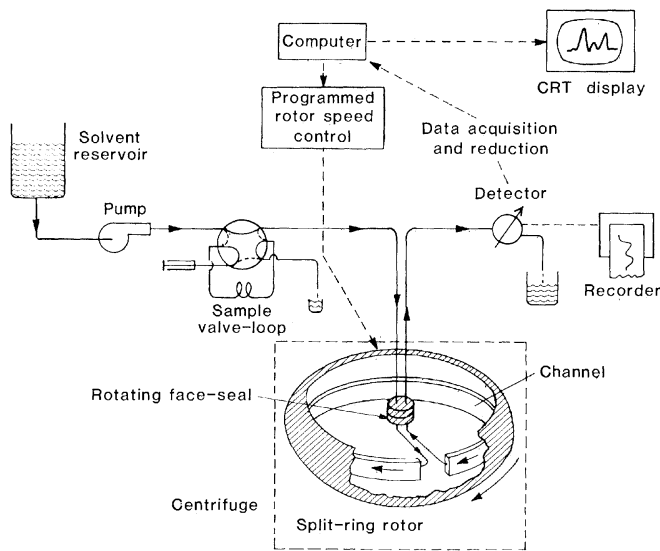


Fig. 6. Schematic of the SFFF apparatus.

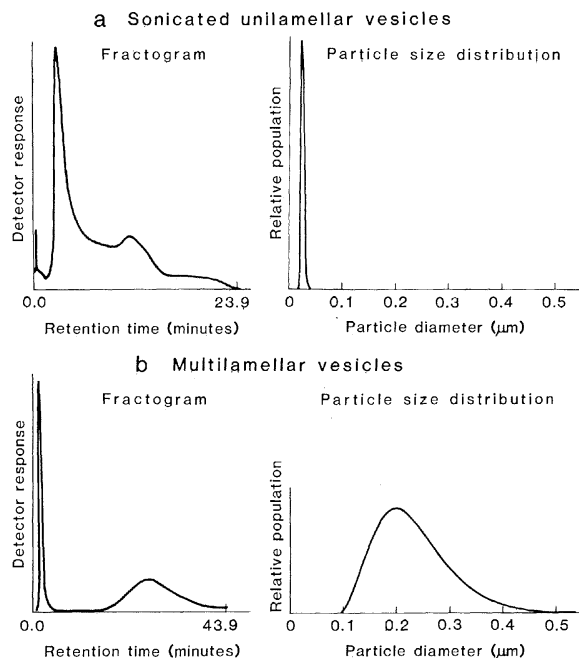


Fig. 7. Characterization of liposome vesicles by time-delay exponential SFFF. Left, fractograms. Right, differential particle size distributions. Channel, 57 by 2.54 by 0.0254 cm. Mobile phase, 0.01M Hepes, 0.142M NaCl, 0.0055M NaOH, pH 7.45 (called HN buffer). Flow rate, 2.0 ml/min. (a) Sonicated unilamellar vesicles. HN buffer plus sugar ($\rho = 1.18$ g/cm³); initial rotor speed, 18,000 rev/min; exponential decay constant, 4.0 minutes; initial time delay, 6.0 minutes; ultraviolet detector, 240 nm. (b) Multilamellar vesicles. Separation conditions same as for (a) with the following exceptions. HN buffer ($\rho = 1.004$ g/cm³); initial time delay, 4.0 minutes; ultraviolet detector, 350 nm.

tion mechanisms and sedimentation distances associated with these two separation methods. In conventional centrifugation, solute banding occurs in a centrifuge tube of limited length. Therefore, centrifugal methods have a limited peak capacity; that is, a limited number of bands can be separated. Increased resolution or peak capacity for smaller or less dense solutes at the top of the tube will result in a loss of resolution or loss of peak capacity near the bottom of the tube for larger or more dense solutes. Peak capacity in SFFF is much larger; resolution and peak capacity for all samples are simultaneously enhanced with increasing gravitational force field, and this is limited only by the maximum field available and practical analysis times. The sedimentation distances required in SFFF separations are about two orders of magnitude smaller than those in the conventional centrifuge separations. Hence, SFFF provides much faster separations.

A simple relation exists between SFFF retention and the sedimentation coefficient

$$\lambda = \frac{D}{S\omega^2 r} \times 10^{13} \quad (7)$$

where λ and ω are as previously defined, D is the diffusion coefficient in centimeters squared per second, and S is the sedimentation coefficient in Svedberg units equivalent to 10^{-13} second.

When the density of the sample is unknown, different carrier liquid densities can be used in different SFFF runs, so that both particle size and particle density can be obtained. Such experiments can be carried out both in constant-field or TDE-SFFF modes. For constant-field SFFF

$$\rho = \rho_s \pm \frac{6kT}{\pi G W d_p^3} \left(\frac{1}{\lambda_\ell} \right) \quad (8)$$

where ρ is the carrier-liquid density in grams per milliliter and λ_ℓ is the corresponding λ value for the carrier liquid of that density. The experimental λ_ℓ value needed here is derived from retention data (Eqs. 3 to 5). A straight line plot of experimental values of ρ versus $1/\lambda_\ell$ gives the intercept corresponding to the solute density ρ_s and the slope corresponding to the particle size parameter of $6kT/\pi G W d_p^3$. The slope is positive when $\rho_s < \rho$ and negative when $\rho_s > \rho$.

For TDE-SFFF

$$\rho = \rho_s \pm \frac{a}{d_p^3} \frac{\tau}{t_0} \exp\left(\frac{t_R}{\tau}\right) \quad (9)$$

where $a = 36kT/\pi e G_0 W$. A straight line plot of experimental ρ versus $[\tau \exp(t_R/\tau)/t_0]$ values provides the intercept corre-

sponding to the solute density ρ_s . The slope ($\pm\alpha/d_p^3$) may be positive or negative depending again on whether $\rho_s < \rho$ or $\rho_s > \rho$, respectively.

Size-exclusion (gel filtration) chromatography. The resolving power of SFFF has been shown to be at least five times that of size-exclusion chromatography (SEC) (10). This difference in separation resolution is the result of the basic differences in the retention mechanisms of the two techniques. For SEC, separation is confined within the available pore volume of the column packing; all solutes elute in a limited retention volume range between total exclusion and total permeation. In contrast, SFFF exhibits retention much like liquid chromatography, with peaks eluting well after the unretained solvent peak. For this reason, SFFF has the potential for very large peak capacity and high resolution, whereas SEC is intrinsically a relatively low-resolution method.

Equipment and Techniques

The general configuration of SFFF equipment is shown schematically in Fig. 6. Details of the apparatus used in the present studies have been described (3, 11). Mobile phase flow was provided by a liquid chromatographic solvent-metering pump, and sample injection was accomplished with a microsampling valve with a replaceable external sample loop. The main SFFF separating system consisted of a specially designed rotating face seal and the SFFF channel housed within a centrifuge. Some of the applications described in this article were carried out with a new SFFF apparatus of a different design (12). A "floating" plastic rotor in an ultracentrifuge (Beckman L5-50B) provided speeds of up to 32,000 rev/min or about 85,000*g*. A microcomputer was used to control rotor speed accurately during exponential programming and to compute particle sizes or molecular weight data from the output of an ultraviolet spectrophotometric detector operated either in the absorption or turbidimetric mode (11).

The general benefits arising from the open-channel configuration used in SFFF have been described (5). Relative to packed beds in liquid chromatography, the open SFFF channel subjects samples to only moderate, usually controllable shear stress, which generally permits samples to be fractionated and collected without alteration. The absence of shear problems in SFFF has been indicated by studies in which virus particles have been fractionated, collect-

ed, assayed, and found viable (13, 14). Additional studies are needed to verify further that SFFF is a very mild fractionating method.

Adsorption of biopolymers to SFFF channel walls has not been a general problem. Migrating sample components are exposed only to a very small surface area, which minimizes solute-surface interaction. In the few quantitative experiments conducted thus far, yields of eluting materials appear to be quantitative. Again, additional studies of this effect are needed.

Like chromatography, SFFF is a continuous flow-separation technique and, as such, demands little attention once the separation is begun. This strongly contrasts to density gradient sedimentation, which requires considerable attention to gradient-forming, sample-loading, and band-eluting steps. About 0.1 to 1.0 milligram of sample can be processed in a single SFFF run without loss of resolution because of channel-overloading effects. However, significantly larger samples (≥ 1 g) can be handled by SFFF with lower resolution (3).

Since the mechanism of SFFF separation is directly related to first principles, molecular weight standards are not needed for the determination of molecular weights or particle size distributions. If

sample and solvent densities are known accurately, the effective mass measured by SFFF can be converted directly into molecular weight or, if the shape is known, into particle dimensions.

Band Broadening

Just as in chromatography, the broadening of zones or bands during migration down an SFFF channel ultimately sets limits on resolution or separation power. The band spreading in SFFF is the result of the steady mass transfer effect of sample components redistributing between slow and fast flow streams across the sample layer near the wall. Since significant time is required for large sample components to be equilibrated across the layer thickness ℓ in the channel, SFFF band broadening is quite significant, at times causing a detection problem. However, in spite of this, SFFF is still a high-resolution separation process because of its large discrimination for species with small mass differences. As expected, increasing the channel thickness W results in increased band broadening (3, 6). Factors such as high retention, thin channel, and low mobile phase velocities generally sharpen the bands and improve resolution.

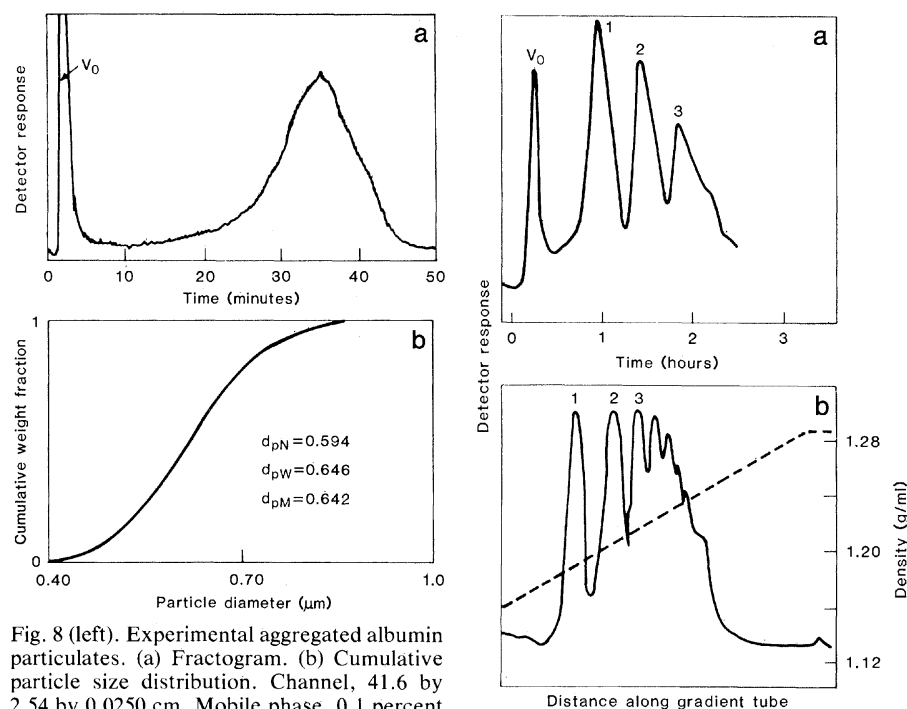


Fig. 8 (left). Experimental aggregated albumin particulates. (a) Fractogram. (b) Cumulative particle size distribution. Channel, 41.6 by 2.54 by 0.0250 cm. Mobile phase, 0.1 percent Aerosol OT. Initial rotor speed, 500 rev/min. Exponential decay constant, 10.0 minutes. Flow rate, 2.0 ml/min. Sample, 100 μl of suspension in normal saline. Turbidimetric detector, 325 nm. Fig. 9 (right). Viral particles from gypsy moth larvae [redrawn from data in (23)]. (a) SFFF fractogram. Channel, 83.3 by 2.0 by 0.0254 cm. Mobile phase flow rate, 0.40 ml/min. Rotor speed (constant), 1417 rev/min. Sample, 100 μl containing about 500 μg . Detector, ultraviolet, 254 nm. (b) Sucrose density gradient centrifugation. Density, 1.283 to 1.127 g/ml (sucrose in 0.01M tris-HAc and 0.001M EDTA, pH 7.4). Centrifugation, 24,000 rev/min for 4 hours. Swinging bucket rotor. Ultraviolet monitor, 254 nm. Sample, 3 ml.

Applications

Particulates. A wide variety of particulates of biochemical interest can be characterized by SFFF. For example, quantitative particle-size distribution analyses of liposomes have been reported (15). This is an important aspect of liposome research because of the increasing use of these particles in drug delivery systems that require a rigorous knowledge of particle size. Figure 7 illustrates the TDE-SFFF of two phospholipid vesicle dispersions; Fig. 7a shows a fractogram of very small sonicated unilamellar vesicles (SUV), and Fig. 7b shows larger multilamellar vesicles (MLV). Cumulative particle size plots of these samples are also shown in Fig. 7 after transformation of turbidimetric detector output to account for the fact that larger particles scatter more light than smaller particles do (11). These data show that the SUV sample has a relatively narrow particle size range, with an average diameter of about 0.026 μm , whereas the MLV exhibits a much wider particle-size distribution, with an average particle-size diameter of about 0.23 μm .

The effects of environment on the conformation of bioparticles can also be studied with SFFF. For example, the MLV in Fig. 7 are osmotically active (16) and should be expected to lose water and shrink in a solution of sugar. Refractionation of the original MLV sample of Fig. 7 in a sucrose buffer mobile phase resulted in a decrease of particle diameter for the MLV particles to 152 nanometers compared to the 232 nm found in the original buffer. This change represents a water loss of 62 percent in the MLV and an increase in particle density to 1.0472 g/cm^3 , compared to the 1.0154 g/cm^3 , the value reported in the literature for the original particles. Particle size analyses with SFFF have also been reported for other liposome preparations (17).

The SFFF method is also useful for obtaining particle size information on experimental particulates of aggregated albumin for liver-imaging studies. Figure 8a shows the fractogram of an aggregated albumin sample obtained with TDE-SFFF. The differential particle size plot of this sample is shown in Fig. 8b where relative particle concentration is plotted against particle diameter after detector output transformation. The particle-size information given in Fig. 8 was obtained by determining the density of the albumin aggregates in the manner described earlier. This SFFF approach provides a convenient method to determine the solvated densities of a wide variety of mac-

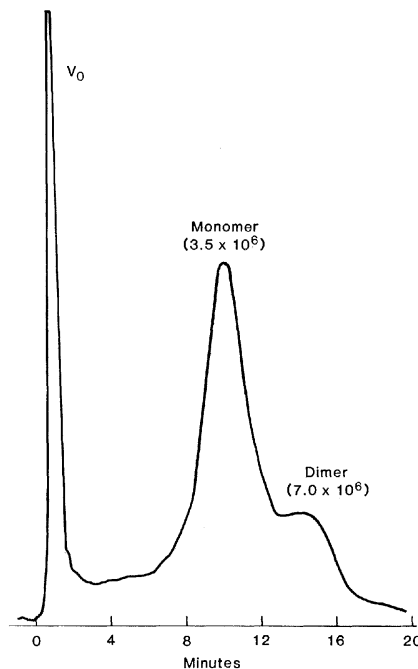


Fig. 10. Fractogram of plasmid pBR325 by time-delay exponential SFFF. Channel, 41.6 by 2.54 by 0.022 cm. Mobile phase, 10 mM each of tris and NaCl, pH 7.6. Initial rotor speed, 25,000 rev/min. Exponential decay constant, 6.0 minutes. Flow rate, 2.0 ml/min. Sample, 13 μg in 100 μl . Ultraviolet detector, 260 nm.

romolecular systems. The aggregated albumin sample was fractionated with mobile phases of varying densities, obtained by adding glycerol to the 0.1 percent Aerosol OT anionic dispersant mobile phase. With this approach, a density of 1.15 g/ml was determined for the aggregates, and this density value was used in calculating the particle size distribution data. The characterization of other albumin microspheres by SFFF has also been reported (18).

The particle size distribution of organic-modified gold colloidal particles has also been characterized with SFFF. These particles have been developed to visualize the ultrasurface of cell surface receptor sites by high-resolution scanning electron microscopy (19, 20). Carbohydrate-specific colloidal gold particles coated with a mixture of glucose and mannose have been proposed for the localization of lectin receptor sites by scanning electron microscopy (21). Particle size distribution analysis of such material (GCP-Con A, E·Y Laboratories) showed a weight-averaged particle size of 18.6 nm. Similarly, gold colloidal particle-linked avidin (GCP-avidin, E·Y Laboratories) used in biotin-avidin systems showed a weight-averaged particle size of 17.8 nm. In both colloidal gold samples, the particle size distributions were relatively narrow, with polydisper-

sities (weight average divided by number average) of about 1.12.

Viruses. Previous SFFF studies have illustrated the ability of this technique to fractionate a variety of viruses. The molecular weights of T-2 (3, 22), T-4D (13), fd (3), QB, and P22 (5) viruses have been reported, and the density of the T-4D virus has also been determined by SFFF (13). Other viruses of biochemical interest have also yielded useful information by SFFF. For example, Fig. 9 demonstrates a SFFF fractogram of a freshly prepared sample of viral particles from lysed inclusion bodies of gypsy moth larvae (23). In this separation the initially eluting void peak contains all sample components with an effective mass of $< 50 \times 10^6$ g/mole. Peak 1, the major peak in Fig. 9, contained a single rodlike enveloped nucleocapsid. Peak 2 of the fractogram contained mostly rodlike dimers whose thickness was more than twice that of the monomer particles. In peak 3, trimers were clearly present, some with visibly intact envelopes and some with the structure partially ruptured.

For comparison, Fig. 9b shows the elution pattern from a sucrose density gradient sedimentation of the same freshly prepared alkali-liberated virus sample. Quantitative definition of the banding in the gradient tube was obtained by ultraviolet absorption.

The SFFF separation in Fig. 9a was arbitrarily concluded shortly after elution of the third peak, and the SFFF shows somewhat better resolution, with much shorter total analysis time than the density gradient centrifugation separation in Fig. 9b. A clean population of enveloped nucleocapsids (peak 1) was obtained in about 30 minutes by SFFF, whereas density gradient sedimentation required more than 4 hours, with considerably more handling problems and inconvenience.

Nucleic acids. The development of SFFF equipment with higher force fields has made possible the examination of a variety of lower molecular weight materials. For example, the plasmid pBR325 preparation in Fig. 10 (Bethesda Laboratories, BRL 5265SA/SB, lot 04112) shows a main constituent with a retention time of about 10 minutes. This retention corresponds to a molecular weight of 3.5×10^6 , compared to the 3.6×10^6 value reported by the supplier. In addition, this preparation exhibited a more strongly retained impurity with a molecular weight of 7.0×10^6 . The relative areas of these two peaks correspond closely to the 60:40 monomer-dimer composition claimed by the supplier.

Still lower molecular weight components may be fractionated by high force field SFFF (12). For example, the single-stranded circular fd viral DNA macromolecule was well retained at 30,000 rev/min (constant field), with peak retention corresponding to a molecular weight of 1.71×10^6 . This closely compares with the reported value of about 1.7×10^6 for this material (24). The protein fibrinogen with a reported molecular weight of 5×10^5 has also been retained with a retention ratio $R = 0.37$, representing the approximate mass limit of separation with our present apparatus (12).

Bacteria. By utilizing low SFFF force fields it is feasible also to fractionate relatively large biomasses, such as *Escherichia coli* bacteria (25).

References and Notes

- J. C. Giddings, M. N. Myers, J. F. Moellmer, *J. Chromatogr.* **149**, 501 (1978).
- J. C. Giddings, S. R. Fisher, M. N. Myers, *Am. Lab.* **10**, 15 (1978).
- J. J. Kirkland, W. W. Yau, W. A. Doerner, J. W. Grant, *Anal. Chem.* **52**, 1944 (1980).
- M. N. Myers, K. A. Graff, J. C. Giddings, *Nucl. Technol.* **51**, 147 (1980).
- J. C. Giddings, M. N. Myers, K. D. Caldwell, S. R. Fisher, *Methods Biochem. Anal.* **26**, 79 (1980).
- J. C. Giddings, F. J. F. Yang, M. N. Myers, *Anal. Chem.* **46**, 1917 (1974).
- G. Karaiskakis, M. N. Myers, K. D. Caldwell, J. C. Giddings, *ibid.* **53**, 1314 (1981).
- W. W. Yau and J. J. Kirkland, *Sep. Sci. Technol.* **16**, 577 (1981).
- J. J. Kirkland and W. W. Yau, U.S. Patent 4,285,810, 25 August 1981.
- W. W. Yau and J. J. Kirkland, *J. Chromatogr.* **218**, 217 (1981).
- J. J. Kirkland, S. W. Rementer, W. W. Yau, *Anal. Chem.* **53**, 1730 (1981).
- J. J. Kirkland, C. H. Dilks, Jr., W. W. Yau, in preparation.
- K. D. Caldwell, G. Karaiskakis, J. C. Giddings, *J. Chromatogr.* **215**, 323 (1981).
- C. D. Crowe and S. D. Abbott, personal communication.
- J. J. Kirkland, W. W. Yau, F. C. Szoka, *Science* **215**, 296 (1982).
- A. D. Bangham, D. de Gier, G. D. Freville, *Chem. Phys. Lipids* **1**, 225 (1976).
- K. D. Caldwell, G. Karaiskakis, J. C. Giddings, *Colloid. Surf.* **3**, 233 (1981).
- K. D. Caldwell, G. Karaiskakis, M. N. Myers, J. C. Giddings, *J. Pharm. Sci.* **70**, 1315 (1981).
- H. Gerber, M. Horisberger, H. Bauer, *Infect. Immun.* **7**, 487 (1974).
- H. Bauer, D. R. Farr, M. Horisberger, *Arch. Microbiol.* **97**, 17 (1974).
- M. Horisberger and J. Rosset, *Experientia* **32**, 998 (1976).
- J. C. Giddings *et al.*, *Sep. Sci.* **10**, 133 (1975).
- K. D. Caldwell, T. T. Nguyen, J. C. Giddings, H. M. Mazzone, *J. Virol. Methods* **1**, 241 (1980).
- H. A. Sober, Ed., *Handbook of Biochemistry*, (Chemical Rubber Co., ed. 2, Cleveland, Ohio, 1970), p. H-4.
- J. J. Kirkland and W. W. Yau, unpublished studies.
- We thank Y-S. E. Cheng of Du Pont for the *Escherichia coli* bacteria, prepared as described in G. H. Miller, *Experiments in Molecular Genetics* (Cold Spring Harbor Laboratory, Cold Spring Harbor, N.Y., 1972).

Reexamination of Acoustic Evidence in the Kennedy Assassination

Committee on Ballistic Acoustics, National Research Council

At the time of the assassination of John F. Kennedy, a microphone, presumably on a police motorcycle, was stuck open and transmitted continuously on Dallas Police Department channel I. The transmissions were recorded on a Dictaphone belt recorder, model A2TC. At the request of the House Select Committee on Assassinations, this belt and magnetic tape copies of it were studied by J. Barger, S. Robinson, E. Schmidt, and J. Wolf (BRSW) of Bolt Beranek and Newman Inc., and later by M. Weiss and E. Aschkenasy (WA) of Queens College. In reports in September 1978 and January 1979, BRSW concluded (1) that the recording contained four sounds, which they attributed to probable gunshots, and that with a probability of 50 percent one of the sounds (the third) was due to a shot from the grassy knoll area of Dealey Plaza in Dallas. Later, WA studied the echo patterns analytically, and their conclusion (1) was that "the odds are less than 1 in 20 that the impulses and echoes were not caused by a gunshot from the grassy knoll, and at least 20 to 1 that they were." BRSW subsequently reviewed the results of WA and concluded (1) that

"the probability that they obtained their match because the two matched patterns were due to the same source (gunfire from the knoll) is about 95%." This conclusion, together with the fact that shots were definitely fired from another location, the Texas School Book Depository, was the basis of the finding by the House Select Committee on Assassinations that "scientific acoustical evidence establishes a high probability that two gunmen fired at President John F. Kennedy."

In response to a request from the Department of Justice, the Committee on Ballistic Acoustics was established by the National Research Council in the fall of 1980 to review the methodology employed in the evaluations of the recorded acoustic data and the conclusions about

the existence of a shot from the grassy knoll. The committee was also asked to recommend the kinds of tests, analyses, and evaluations needed to obtain better information from the recording.

In the first months of its existence, the committee studied the analytical techniques used by BRSW-WA. Committee members found errors in the previous studies which were sufficiently serious that, by the end of the first committee meeting, no member was convinced by previous acoustic analyses that there was a grassy knoll shot.

The committee continued its studies to challenge its own conclusion and search for additional acoustic evidence. In particular, it followed up a suggestion that cross talk from Dallas Police Department channel II was weakly recorded with the sounds attributed to gunfire on channel I. On the day of the assassination, channel I was primarily used for normal police activities. Channel II was used for the presidential motorcade and was recorded on a Gray Audograph disk. The quality of the cross talk on the recording from channel I was so poor that the committee could not conclude by listening to the recordings from the two channels that the two messages were the same. Hence it made sound spectrograms of portions of the two recordings. Analyses of the spectrograms showed

The Committee on Ballistic Acoustics includes Norman F. Ramsey, Harvard University, chairman; Luis W. Alvarez, Lawrence Berkeley Laboratory, University of California; Herman Chernoff, Massachusetts Institute of Technology; Robert H. Dicke, Princeton University; Jerome I. Elkind, Xerox Palo Alto Research Center; John C. Feggeler, Bell Laboratories, Holmdel, New Jersey; Richard L. Garwin, Thomas J. Watson Research Center, IBM Corporation, and Department of Physics, Columbia University; Paul Horowitz, Harvard University; Alfred Johnson, Bureau of Alcohol, Tobacco, and Firearms, National Laboratory Center, Department of the Treasury; Robert A. Phinney, Princeton University; Charles Rader, Lincoln Laboratory, Massachusetts Institute of Technology; and F. Williams Sarles, Trisolator Corporation, Bedford, Massachusetts. Staff members at the National Research Council are C. K. Reed and Bertita E. Compton, Commission on Physical Sciences, Mathematics, and Resources. This article is based on the committee's formal report, which will be released in November 1982.